

THEORETICAL
AND MATHEMATICAL PHYSICS

Thermal Monopoles in the $SU(2)$ Gauge Theory on a Lattice

V. G. Bornyakov^{a, b} and A. G. Kononenko^c

^a Institute of High-Energy Physics, pl. Nauki 1, Protvino, Moskovskaya oblast, 142280 Russia

^b Institute for Theoretical and Experimental Physics, ul. Bol'shaya chermushkinskaya 25, Moscow, 117218 Russia

^c Department of Physics, Moscow State University, Moscow, 119991 Russia

e-mail: vitaly.bornyakov@ihep.ru, agkono@gmail.com

Received January 8, 2014; in final form, March 6, 2014

Abstract—Color-magnetic thermal monopoles in $SU(2)$ lattice gluodynamics with improved Simanzik action were studied. The density of the monopoles, the monopole chemical potential, the cluster susceptibility, and the cluster magnetization were studied. These results were compared with results that were reported elsewhere.

Keywords: lattice gauge theories, confinement–deconfinement transition, Abelian color-magnetic monopoles, Bose–Einstein condensation, maximum Abelian gauge, Gribov copies.

DOI: 10.3103/S0027134914040055

INTRODUCTION

In recent works on the collision of heavy ions it has been found that quark–gluon matter is a medium with strong interaction [1]. In [2, 3], it was proposed that the unusual properties of quark–gluon matter, including a very low ratio of the viscosity to the entropy density, can be explained via the consideration of color-magnetic monopoles. The first works on investigating the role of these degrees of freedom in a quark–gluon medium using lattice methods were described in [5–11].

In our earlier work [12], we investigated the universality of the properties of thermal monopoles, i.e., their independence of the selection of a lattice action. Studies of Abelian color-magnetic currents at the zero temperature have shown that the density of the infrared component of the magnetic current for various lattice actions changes by $\sim 30\%$ [13]. This means that ultraviolet fluctuations make a contribution to the infrared density and should be suppressed. The partial suppression of these fluctuations was achieved by using an improved action. In [12], we used an improved Simanzik lattice action and compared our results for the density and the other characteristics with the results that were obtained using the Wilson action [7–9, 11]. It was found that for thermal monopoles universality was satisfied if short-range (ultraviolet) dipoles were not considered.

In this work, we continue to study the properties of thermal monopoles with an improved lattice action in the $SU(2)$ gauge theory with specific attention to changes in the properties of thermal monopoles in the vicinity of the confinement–deconfinement phase transition. Quantitatively exact determination of

parameters, such as the density of monopoles and the magnetic coupling constant, is necessary, in particular, to verify the hypothesis that magnetic monopoles weakly interact (compared to electrically charged fluctuations) just above the phase transition, but strongly interact at high temperatures [2]. To eliminate the systematic effects caused by Gribov copies, in this work, we used the same procedure for gauge fixing as was applied in [10–12].

1. MODELING DETAILS

The lattice action we used is written as follows:

$$S = \beta_{impr} S_{pl} - \frac{\beta_{impr}}{20u_0} \sum_{rt} S_{rt}, \quad (1)$$

where $\beta_{impr} = 4/g^2$ is the inverse coupling constant, u_0 is the parameter of the additional term, and S_{pl} and S_{rt} are the plaquette and rectangular 1×2 loop summands in the action, respectively:

$$S_{pl, rt} = \frac{1}{2} \text{Tr}(1 - U_{pl, tr}), \quad u_0 = \sqrt[4]{\frac{1}{2} (\text{Tr}(U_{pl}))}. \quad (2)$$

The calculations were carried out using an asymmetric lattice with the volume $V = L_t \times L_s^3$ and the periodic boundary conditions, where $L_t = 6$ and $L_s = 48$ are the numbers of sites in the time and spatial directions, respectively. The temperature was assigned using the following relationship:

$$T = \frac{1}{aL_t}, \quad (3)$$

Table 1. Values of β_{imp} , the parameter u_0 , and the temperature, as well as the number of configurations that were used. T_c is the temperature at the phase transition point

β_{imp}	u_0	T/T_c	N_{meas}
3.480	0.91681	1.50	200
3.400	0.91402	1.31	372
3.340	0.91176	1.20	260
3.313	0.91056	1.13	228
3.300	0.91015	1.10	203
3.285	0.90954	1.07	306
3.265	0.90867	1.03	416
3.230	0.90714	0.97	238
3.215	0.90646	0.94	300
3.200	0.90578	0.91	201
3.100	0.90069	0.76	100

where a is the lattice spacing. To determine the value of u_0 , we used the results of [13] either directly or by performing an interpolation to the required value.

The maximum Abelian gauge was fixed by finding the maximum of the gauge functional [14, 15]

$$F_U(g) = \frac{1}{4V} \sum_{x, \mu} \frac{1}{2} \text{Tr}(U_{g, \mu}^g \sigma_3 U_{g, \mu}^{g, \dagger} \sigma_3) \quad (4)$$

with respect to the gauge transformations of the lattice gauge field $U_{x, \mu}$

$$U_{x, \mu} \longrightarrow U_{x, \mu}^g = g_x U_{x, \mu} g_{x+\mu}^\dagger. \quad (5)$$

To determine the monopole currents, after the gauge has been fixed, the Abelian projection was implemented; as a result, the Abelian phase $\theta_\mu(x)$ was extracted from the non-Abelian variable $U_{x, \mu}$ and the Abelian plaquette $\theta_{\mu\nu}(x)$ was then constructed using the following formula:

$$\begin{aligned} \theta_{\mu\nu} &= \theta_\mu(n) + \theta_\nu(n + \hat{\mu}) - \theta_\mu(n + \hat{\nu}) \\ &- \theta_\nu(n) = \bar{\theta}_{\mu\nu} + 2\pi m_{\mu\nu}, \end{aligned} \quad (6)$$

where $\bar{\theta}_{\mu\nu} \in (-\pi, \pi]$ is the compactified component of the Abelian plaquette phase. Finally, the Abelian monopole currents were determined using the following construction [16]:

$$j_\mu(x) = \frac{1}{2\pi} \varepsilon_{\mu\nu\alpha\beta} \hat{\partial}_\nu \bar{\theta}_{\alpha\beta}(x). \quad (7)$$

The monopole currents were determined on links $\{x, \mu\}^*$ of the dual lattice and take on integer values $j_\mu(x) = 0, \pm 1, \pm 2$. Since the law of conservation $\hat{\partial}_\mu j_\mu(x) = 0$ is obeyed, the monopole currents form closed loops, which make up clusters. A part of the clusters (at the zero temperature, all clusters) are

closed within volume; however, some clusters are closed through the boundary of the lattice in the time direction. The degree of winding N_{wr} of such a cluster is determined by the following relationship:

$$N_{wr} = \frac{1}{L_t} \sum_{j_4(x) \in \text{cluster}} j_4(x). \quad (8)$$

These clusters were first studied in [4, 17].

To capture the maximum Abelian gauge, the stimulated annealing algorithm was used, which turned out to be very efficient for this gauge [18]. In order to reduce the effect of Gribov copies even more, ten Gribov copies were constructed for each configuration of the lattice gauge field; each time we started from the procedure of the fixing of a gauge from a randomly chosen gauge copy of the initial Monte-Carlo configuration.

Table 1 presents the information on the ensemble of gauge fields and the parameters used in this work.

2. CONDENSATION OF MONOPOLES

In this section, we consider thermal monopoles with various values of the number of windings N_{wr} . In [9], it was proposed to use these trajectories to assess the Bose condensation of thermal monopoles when the temperature is decreased to a critical value. The central idea of this approach can be formulated as follows.

In the path integral, which describes the system of N identical particles, the trajectory of each particle should be closed in the time direction owing to the periodic boundary conditions, but up to the permutation of N particles. This means that an ensemble of N identical particles is not necessarily made up of N single closed trajectories; it may consist of $M < N$ trajectories provided that some of these trajectories are closed through the time direction more than once. Thus, for an arbitrary configuration that describes N identical particles with $M < N$ trajectories, the following relationship is obeyed:

$$\sum_{k=1}^{k_{\max}} N_k k = N, \quad \sum_{k=1}^{k_{\max}} N_k = M, \quad (9)$$

where N_k is the number of trajectories with k windings.

This property of an ensemble of identical particles can be used to assess quantum statistical effects. If a system is close to the Boltzmann approximation, the contributions of trajectories with more than one winding are suppressed. On the other hand, the appearance of trajectories with a progressively increasing number of windings is indicative of more-pronounced quantum effects, which should be the case at temperatures close to the temperature of Bose condensation.

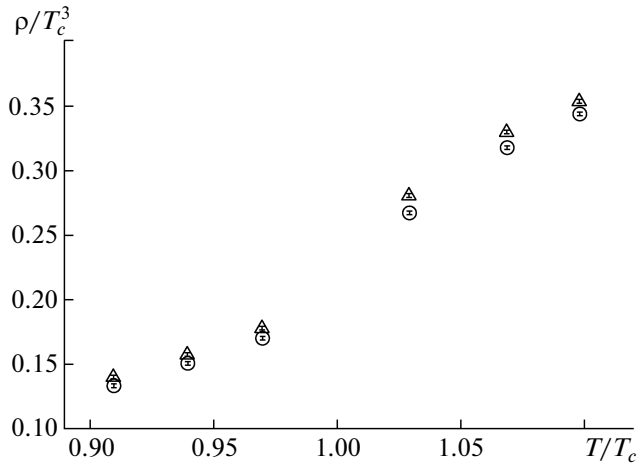


Fig. 1. The temperature dependences of the total density of the monopoles ρ/T_c^3 (triangles) and the density of clusters with a single winding, ρ_1/T_c^3 (circles).

A description of these properties of the ensemble of identical particles on the lattice is as follows.

The density of the thermal monopoles is determined by the following expression:

$$\rho = \frac{\langle \sum_{\text{clusters}} |N_{wr}| \rangle}{L^3 a^3}. \quad (10)$$

It is known that for the ideal Bose gas [9, 20], the density of trajectories with number of windings k can be written as follows:

$$\rho_k = \frac{e^{-\hat{\mu}k}}{\lambda^3 k^{5/2}}, \quad (11)$$

where $\hat{\mu} \equiv -\mu/T$; μ is the chemical potential and λ is the de Broglie thermal wavelength. The temperature of condensation is determined by the equality of the chemical potential to zero.

When analyzing the monopole density ρ_k in the vicinity of T_c , it was found that its values for $k = 1, 2$ sharply rose at the transition from the confinement phase ($T < T_c$) to the deconfinement phase ($T > T_c$). This behavior can be seen in Figs. 1 and 2. This phenomenon was discovered for the first time. Thus, the densities ρ_1 and ρ_2 , as well as the total density ρ , which is also shown in Fig. 1, are the indicators of the confinement–deconfinement transition.

Figure 2 also shows the density ρ_3 , which exhibits a substantially less pronounced increase. It can be assumed that with increasing k the discovered effect rapidly becomes weaker.

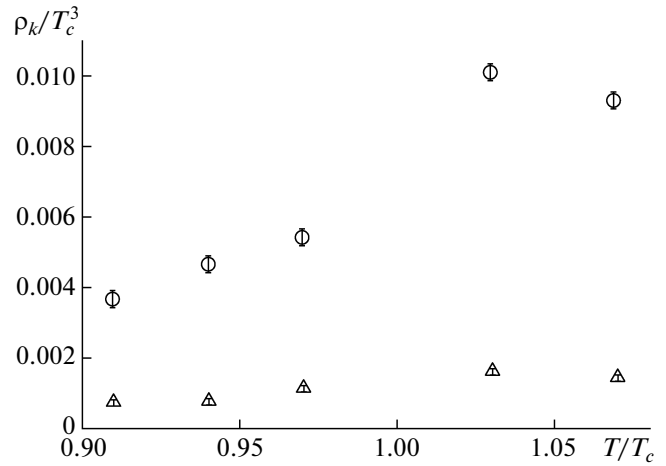


Fig. 2. The temperature dependences of the densities of the monopoles ρ_2/T_c^3 (circles) and ρ_3/T_c^3 (circles).

To take the interaction between the monopoles into account, the authors of [9] proposed to modify Eq. (11) to the following equation

$$\frac{\rho_k}{T^3} = \frac{Ae^{-\hat{\mu}k}}{k^\alpha}, \quad (12)$$

with the free parameter α . The condensation of the monopoles occurs when the effective chemical potential becomes zero.

We approximated the obtained data for $\frac{\rho_k}{T^3}$ by

Eq. (12) in the range of temperatures close to T_c . Four values of the parameter α were assigned. Figure 3 shows the dependence of ρ_k/T^3 on k together with the

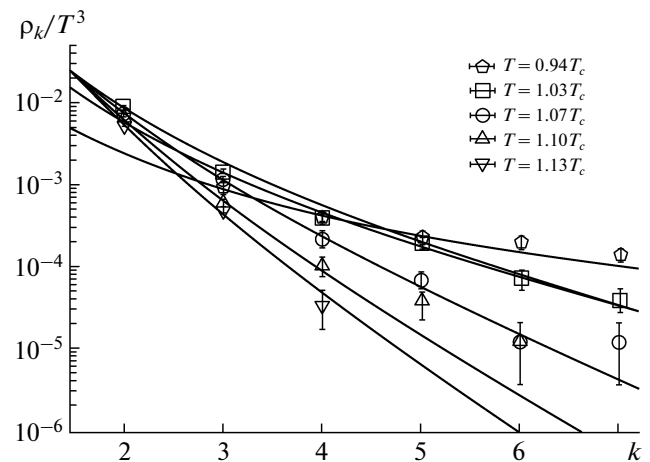


Fig. 3. The dependences of the density of the monopoles ρ_k/T^3 on the number of windings of the monopole trajectory, k . The lines show the approximations for $\alpha = 2.5$.

Table 2. Values of the parameters of the effective chemical potential $\hat{\mu}$ that were obtained for four values of the parameter α by approximating the dependence ρ_k/T^3 by Eq. (12) with the corresponding χ^2/n_{df}

T	$\alpha = 0$		$\alpha = 2$		$\alpha = 2.5$		$\alpha = 3$	
	$\hat{\mu}$	χ^2/n_{df}	$\hat{\mu}$	χ^2/n_{df}	$\hat{\mu}$	χ^2/n_{df}	$\hat{\mu}$	χ^2/n_{df}
$0.91T_c$	0.55(6)	0.93	0.09(3)	0.44	-0.02(3)	0.42	-0.14(3)	0.44
$0.94T_c$	0.34(3)	2.03	0.05(2)	1.07	-0.02(2)	1.30	-0.08(2)	1.71
$0.97T_c$	0.43(5)	2.49	0.09(2)	0.96	0.01(2)	0.94	0.56(4)	1.09
$1.03T_c$	1.04(9)	2.88	0.53(6)	1.31	0.41(5)	1.01	0.29(4)	0.77
$1.07T_c$	1.79(7)	1.42	1.04(4)	0.55	0.86(4)	0.45	1.03(8)	0.44
$1.10T_c$	2.2(1)	2.27	1.4(1)	1.84	1.2(1)	0.45	1.28(2)	1.61
$1.13T_c$	2.42(7)	0.40	1.65(3)	1.33	1.47(1)	1.73	1.94	2.04
$1.20T_c$	3.15		2.34		2.14			

approximations for the case $\alpha = 2.5$. The results of the approximations for all values of α are presented in Table 2. For the statistics we dealt with, the parameter α could be considered as a free parameter only when approximating the data in the confinement phase; if it was assumed that $\mu = 0$, the parameter α took on the values of 2.1–2.5.

Figure 4 shows the temperature dependence of the chemical potential at $\alpha = 2.5$. It can be seen that with a decrease in the temperature from $1.2T_c$ to $1.03T_c$, the chemical potential diminishes and reaches a value of ~ 0.4 , which qualitatively agrees with the theoretical predictions for a Bose condensation. At temperatures below T_c , the values of the chemical potential agree with the zero value within the statistical error, as expected. The chemical potential in the confinement phase was calculated for the first time.

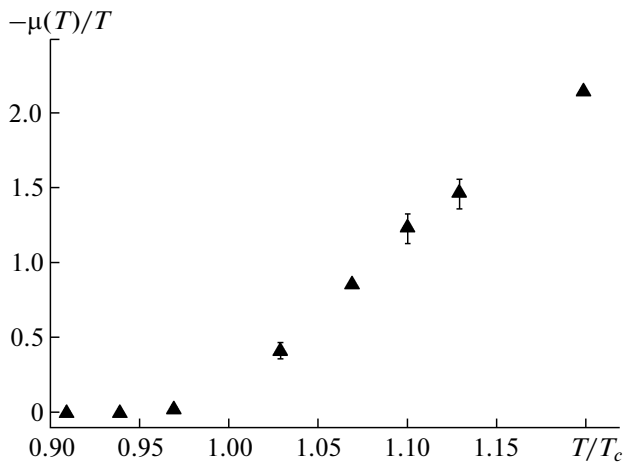


Fig. 4. The temperature dependence of the cluster chemical potential, $-\mu/T$.

3. CLUSTER PERCOLATION

In this section, a cluster percolation transition is considered. As mentioned in section 1, the monopole currents make up clusters. The pattern of the distribution of the clusters over the volume of the lattice depends on the temperature. It was first shown in [4] that in the confinement phase there was always a large (percolating) cluster, which included a substantial fraction of the monopole currents. At temperatures above the temperature of the transition to the deconfinement phase that cluster vanished.

In this work, we carried out the same calculations as those performed in [4], but with a much higher accuracy, i.e., with much lower statistical (our statistics were substantially more extensive than those in [4]) and systematic errors (the volume of the lattice was increased, the lattice spacing was reduced, the gauge fixing was improved, and an improved action was used). The aim was to confirm the conclusion drawn in [4] that the percolation transition of the monopole currents coincides with the confinement–deconfinement phase transition using a much higher accuracy of numerical calculations.

There are various definitions of a percolating cluster [19]. In this work, a cluster was deemed to be percolating if it embraced the entire volume of the lattice but could contain voids. The appearance of a percolating cluster in percolation theory is a phase transition that is characterized by the critical temperature T_c .

Using lattice methods, the temperature at which the percolation transition occurs can be determined by calculating two quantities that characterize the distribution of clusters over the volume of the lattice, i.e., the cluster susceptibility χ_{cl} and the cluster magnetization P_{cl} (these quantities are named by analogy with

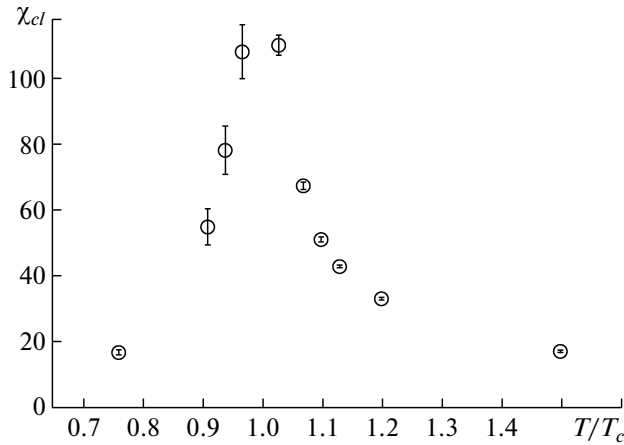


Fig. 5. The temperature dependence of the cluster susceptibility, χ_{cl} .

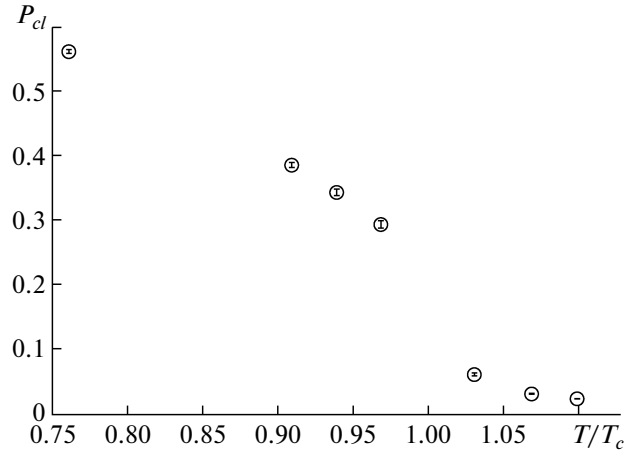


Fig. 6. The temperature dependence of the cluster magnetization, P_{cl} .

spin systems [20]). The cluster susceptibility is determined using the following relationship:

$$\chi_{cl} = \frac{\sum_{N=4}^{N_{\max}} (g(N)N^2) - N_{\max}^2}{N_{\text{tot}}}, \quad (13)$$

where N_{tot} is the total number of sites in all clusters for the given configuration, N_{\max} is the number of sites in the largest cluster, and $g(N)$ is the weight of the cluster with size N . Summation is carried out over the clusters of all sizes from the smallest ($N = 4$) to the largest (N_{\max}). It can be seen from Eq. (13) that χ_{cl} is the average size of a cluster, except for the largest one. The value of χ_{cl} was first calculated on small lattices in [4]. Figure 5 shows the temperature dependence of χ_{cl} . It can be seen that at $T = 1.5T_c$ the lattice is filled with clusters with an average size of 17 sites per cluster. With a decrease in temperature to T_c , the average cluster size rapidly increases and reaches a value of 112 sites per cluster at $1.03T_c$. At the percolation transition point, χ_{cl} has the maximum value, which tends to infinity in the infinite volume limit. At temperatures below T_c , the average size of a nonpercolating cluster sharply drops and, on reaching a temperature of $0.76T_c$, it again becomes equal to ~ 16 sites per cluster.

The cluster magnetization is determined using the following relationship:

$$P_{cl} = \frac{N_{\max}}{N_{\text{tot}}}, \quad (14)$$

where N_{\max} and N_{tot} have the same meanings as in expression (13). The dependence of P_{cl} on T is shown in Fig. 6. It can be seen that at temperatures that slightly exceed T_c the largest cluster contains less than 10% of all sites of the configuration. On transition

through T_c , P_{cl} rapidly increases with decreasing temperature and reaches a value of more than 55% at $T = 0.76T_c$. Thus, the behavior of P_{cl} is typical of the order parameter.

The data in Figs. 5 and 6 confirm the well-known fact that the percolation transition of the monopole clusters coincides with the phase transition. Since our calculations are carried out on large lattices and for a fairly small lattice spacing (in the vicinity of the phase transition, the lattice size is ≈ 5.2 fm and the lattice spacing is $a \approx 0.11$ fm), these results show that the conclusion of the coincidence of these transitions remains valid in the infinite volume limit and in the infinite cutoff limit (at the zero lattice spacing).

We note that no calculations were carried out at $T = T_c$ to avoid finite-volume effects and the effects of correlation between our lattice configurations, which were more pronounced at the transition point. When calculating χ_{cl} and P_{cl} at temperatures close to T_c , the following effects of the lattice finite size were observed. At $T < T_c$, in addition to the largest cluster, whose size substantially exceeded the sizes of the other clusters, one or two clusters, whose sizes were $\approx 1/3$ – $1/5$ of the size of the percolating cluster, were observed in each configuration. In these cases, a specific feature of these clusters (including the largest one) was that they had a nonzero winding along the spatial direction and were the boundary of one and the same surface made up of Dirac plaquettes, i.e., plaquettes with nonzero values of $m_{\mu\nu}$. These clusters were considered as fragments of the percolating cluster and their sites were included in the number of sites that belonged to the percolating cluster. Such finite-volume effects were discovered earlier at $T = 0$ [13].

These results show that a sharp rise in the density of the thermal monopoles at $T \approx T_c$ results from the decomposition of the percolating cluster. The interest-

ing issue of the relationship between the phenomenon of the Bose condensation of thermal monopoles and the phenomenon of the percolation of magnetic currents requires additional study.

CONCLUSIONS

The properties of thermal color-magnetic monopoles and the percolation transition of color-magnetic currents were studied using an improved lattice action (1) and an adequate procedure of gauge fixing. The results confirm the fact that thermal magnetic monopoles are infrared fluctuations rather than artefacts of gauge fixing. The following results were obtained for the first time: (1) the density of the thermal monopoles rapidly increases with increasing temperature near T_c ; therefore, it can serve as an indicator of the confinement–deconfinement transition; this sharp rise in the density results from an increase in the density of the thermal monopoles with $k = 1$; (2) the chemical potential for the thermal monopoles in the confinement phase is equal to zero, as expected; and (3) our data (see Figs. 5 and 6) show that the percolation transition of the monopole clusters coincides with the phase transition to the deconfinement phase in the infinite volume limit and in the infinite cutoff limit (at zero lattice spacing). Currently, we are performing investigations of $SU(3)$ gluodynamics and quantum chromodynamics.

REFERENCES

1. J. Adams, M. M. Aggarwal, Z. Ahammed, J. Amonett, B. D. Anderson, D. Arkhipkin, G. S. Averichev, S. K. Badyal, Y. Bai, J. Balewski, O. Barannikova, L. S. Barnby, J. Baudot, S. Bekele, V. V. Belaga, A. Bellingeri-Laurikainen, R. Bellwied, J. Berger, B. I. Bezverkhny, S. Bharadwaj, A. Bhasin, A. K. Bhati, V. S. Bhatia, H. Bichsel, J. Bielcik, J. Bielcikova, A. Billmeier,

- L. C. Bland, C. O. Blyth, B. E. Bonner, M. Botje, and A. Boucham, *Nucl. Phys. A* **757**, 102 (2005).
2. J. Liao and E. Shuryak, *Phys. Rev. C* **75**, 054907 (2007).
3. M. N. Chernodub and V. I. Zakharov, *Phys. Rev. Lett.* **98**, 082002 (2007).
4. V. G. Borniyakov, V. K. Mitryushkin, and M. Muller-Preussker, *Phys. Lett. B* **284**, 99 (1992).
5. E. Shuryak, *Prog. Part. Nucl. Phys.* **62**, 48 (2009).
6. C. Ratti and E. Shuryak, *Phys. Rev. D: Part., Fields, Grav. Cosmol.* **80**, 034004 (2009).
7. A. D' Alessandro and M. D' Elia, *Nucl. Phys. B* **789**, 241 (2008).
8. J. Liao and E. Shuryak, *Phys. Rev. Lett.* **101**, 162302 (2008).
9. A. D' Alessandro, M. D' Elia, and E. V. Shuryak, *Phys. Rev. D: Part., Fields, Grav. Cosmol.* **81**, 094501 (2010).
10. V. Borniyakov and V. Braguta, *Phys. Rev. D: Part., Fields, Grav. Cosmol.* **84**, 074502 (2011).
11. V. Borniyakov and V. Braguta, *Phys. Rev. D: Part., Fields, Grav. Cosmol.* **85**, 014502 (2012).
12. V. G. Borniyakov and A. G. Kononenko, *Phys. Rev. D: Part., Fields, Grav. Cosmol.* **86**, 074508 (2012).
13. V. Borniyakov, E. -M. Ilgenfritz, and M. Mueller-Preussker, *Phys. Rev. D: Part., Fields, Grav. Cosmol.* **72**, 054511 (2005).
14. A. S. Kronfeld, M. Laursen, G. Schierholz, and U. Wiese, *Phys. Lett. B* **198**, 516 (1987).
15. G. Hooft, *Nucl. Phys. B* **190**, 455 (1981).
16. A. de Grand and D. Toussaint, *Phys. Rev. D: Part., Fields, Grav. Cosmol.* **22**, 2478 (1980).
17. S. Ejiri, *Phys. Lett. B* **376**, 163 (1996).
18. G. S. Bali, V. Borniyakov, M. Muller-Preussker, and K. Schilling, *Phys. Rev. D: Part., Fields, Grav. Cosmol.* **54**, 2863 (1996).
19. G. Damm and W. Kerler, *Phys. Lett. B* **397**, 216 (1997).
20. M. Adrian and J. Schakel, *Phys. Rev. E* **63**, 026115 (2001).

Translated by D. Tkachuk